Synthesis and Characterization of Two Isomers of Decacarbonyl(1,4-dialkyl-1,4-diaza-1,3-butadiene)triosmium: $Os_3(CO)_{10}$(R-DAB).[1] Fluxional Behavior of $Os_3(CO)_{10}$(*i*-Pr-DAB(4e)). Molecular Structures of the 48e Cluster $Os_3(CO)_{10}$(*i*-Pr-DAB(4e)) and of the 50e Cluster $Os_3(CO)_{10}$(c-Pr-DAB(6e)) Containing a 4e Donor σ,σ-N,N′ and a 6e Donor σ-N, μ_2-N′, η^2-C=N′ Bonded R-DAB Ligand, Respectively

Robert Zoet, Johann T. B. H. Jastrzebski, Gerard van Koten, Taasje Mahabiersing, and Kees Vrieze*

Anorganisch Chemisch Laboratorium, University of Amsterdam, Nieuwe Achtergracht 166, 1018 WV Amsterdam, The Netherlands

Dick Heijdenrijk and Casper H. Stam

Laboratorium voor Kristallografie, University of Amsterdam, Nieuwe Achtergracht 166, 1018 WV Amsterdam, The Netherlands

Received November 24, 1987

$Os_3(CO)_{10}(MeCN)_2$ reacts at room temperature with 1,4-disubstituted-1,4-diaza-1,3-butadiene (R-DAB)[1b] to yield two isomers (**1** and **2**) of $Os_3(CO)_{10}$(R-DAB). The product ratio depended on the R group and in one case on the polarity of the solvent. When R = neo-Pent, $Os_3(CO)_{10}$(neo-Pent-DAB(4e)) (**1c**) was isolated, whereas with R = c-Pr, $Os_3(CO)_{10}$(c-Pr-DAB(6e)) (**2a**) was the only product. In the case of R = *i*-Pr reactions in MeCN and THF gave $Os_3(CO)_{10}$(*i*-Pr-DAB(4e)) (**1b**), whereas the reaction in toluene afforded $Os_3(CO)_{10}$(*i*-Pr-DAB(6e)) (**2b**). The structure in the solid state of both isomers (**1b** and **2a**) has been determined. Crystals of $Os_3(CO)_{10}$(*i*-Pr-DAB(4e)) (isomer **1**) are triclinic, space group $P\bar{1}$, with a = 10.777 (2) Å, b = 13.562 (2) Å, c = 8.426 (2) Å, α = 98.92 (2)°, β = 96.45 (2)°, γ = 90.00 (2)°, and Z = 2. The structure was solved via the heavy-atom method and refined to R = 0.047 and R_w = 0.097 by using 3949 independent reflections above the $3\sigma(I)$ level. The structure consists of a $Os_3(CO)_{10}$ unit to which a R-DAB ligand is chelate (4e) bonded. One N atom occupies an axial site and the other an equatorial site [Os(1)-N(1) = 2.07 (1) Å and Os(1)-N(2) = 2.11 (1) Å]. The C=N bonds are slightly lengthened compared to the free ligand [C=N = 1.30 (3) Å (mean)] while the central C-C′ bond is slightly shortened [C(11)-C(12) = 1.41 (2) Å]. Variable-temperature ^{13}C (125 MHz) and ^1H NMR (500 MHz) experiments for **1b** and **1c** demonstrated that there are at least three fluxional processes for **1b** depending on the temperature range. From 193 K a rocking motion of the R-DAB ligand is observed above the osmium triangle about one axial and two equatorial sites on one osmium atom. Above 203 K a second process is observed involving pairwise bridge–terminal carbonyl interchanges perpendicular to the plane of the osmium triangle, while above 293 K various processes occur whereby all carbonyls are scrambled. Crystals of $Os_3(CO)_{10}$(c-Pr-DAB(6e)) (isomer **2**) are triclinic, space group $P\bar{1}$, with a = 9.775 (3) Å, b = 13.730 (4) Å, c = 9.222 (5) Å, α = 107.39 (3)°, β = 101.04 (5)°, γ = 87.84 (3)°, and Z = 2. The structure was solved via the heavy-atom method and refined to R = 0.052 and R_w = 0.059 by using 4243 independent reflections above the $2.5\sigma(I)$ level. The molecule contains a bridging 6e donating R-DAB ligand, bonded in the σ-N, μ_2-N′, η^2-C=N′ coordination mode: σ-N to Os(1) [Os(1)-N(1) = 2.12 (1) Å], symmetrically μ_2-N′ bridging Os(1) and Os(2) [Os(1)-N(2) = 2.12 (1) Å and Os(2)-N(2) = 2.12 (1) Å], and η^2-C=N′ bonded to Os(2) by means of the C(2)-N(2) π-bond of the imine system [Os(2)-C(2) = 2.14 (2) Å]. This 50e cluster comprises an opened metal polyhedron with two normal Os-Os bonds [Os(1)-Os(3) = 2.931 (3) Å and Os(2)-Os(3) = 2.928 (5) Å] and a nonbonding Os(1)···Os(2) distance of 3.591 (3) Å. Os(1) and Os(2) are held together by the bridging ligand. The Os(1)-Os(3)-Os(2) angle is 75.6 (1)°.

Introduction

Part of the work in our laboratory is focused on a study of the synthesis of mono-, bi-, and polynuclear iron, ruthenium, and osmium carbonyl R-DAB[1b] complexes[2-4] as well as of the coordination behavior and chemical activation of the R-DAB ligand in these complexes.

The reactions of R-DAB with $Ru_3(CO)_{12}$ showed a rich chemistry, part of which is presented in Scheme I.[5,6] The first step in these reactions comprises a breakdown of the Ru_3 cluster to $Ru(CO)_3$(R-DAB(4e)), which is followed by a rebuilding into $Ru_2(CO)_6$(R-DAB(6e)) and via $Ru_2(CO)_5$(R-DAB(8e)) into $Ru_3(CO)_9$(R-DAB(8e)) and Ru_3-

(1) (a) Part 1. For part 2 see ref 12. (b) 1,4-Disubstituted-1,4-diaza-1,3-butadienes, RN=C(H)C(H)=NR, are abbreviated as R-DAB. The number of electrons donated by the R-DAB ligand to the cluster is indicated in parentheses: i.e., R-DAB(4e) stands for σ,σ-N,N′ chelating, 4e coordinated; R-DAB(6e) stands for σ-N, μ_2-N′, η^2-C=N′ bridging, 6e coordinated; R-DAB(8e) stands for σ,σ-N,N′, η^2,η^2-C=N,C′=N′ bridging, 8e coordinated. (c) Pyridine-2-carbaldimines, C_5H_4N-2-C(H)=NR, are abbreivated as R-Pyca.

(2) van Koten, G.; Vrieze, K. *Adv. Organomet. Chem.* **1982**, *21*, 151.

(3) Vrieze, K. *J. Organomet. Chem.* **1986**, *300*, 307.

(4) Vrieze, K.; van Koten, G. *Inorg. Chim. acta* **1985**, *100*, 79.

(5) Keijsper, J.; van Koten, G.; Polm, L. H.; Vrieze, K. *Inorg. Chem.* **1984**, *23*, 2142.

(6) Keijsper, J.; Polm, L. H.; Seignette, F. A. B.; Stam, C. H.; van Koten, G.; Vrieze, K. *Inorg. Chem.* **1985**, *24*, 518.

0276-7333/88/2307-2108$01.50/0

Scheme I. The $Ru_3(CO)_{12}$/R-DAB Reaction Sequence

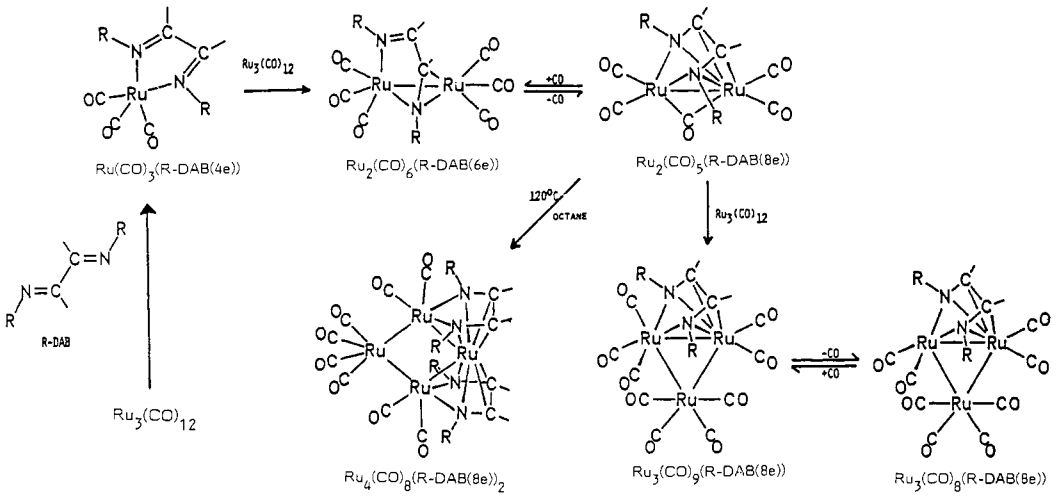

$(CO)_8$(R-DAB(8e)). In these complexes the R-DAB ligand shows a versatile coordination behavior, ranging from 4e σ,σ-N,N′ in $Ru(CO)_3$(R-DAB(4e)) and 6e σ-N, μ_2-N′, η^2-C=N′ in $Ru_2(CO)_6$(R-DAB(6e)) to 8e σ,σ-N,N′, η^2,η^2-C=N,C′=N′ in $Ru_2(CO)_5$(R-DAB(8e)), $Ru_3(CO)_9$(R-DAB(8e)), $Ru_3(CO)_8$(R-DAB(8e)), and $Ru_4(CO)_8$(R-DAB(8e))$_2$. However, the reaction steps and trinuclear ruthenium carbonyl R-DAB intermediates formed in the initial stages of the reaction, which proceed the cluster breakdown, remained obscure since these intermediates could never be isolated.

Reactions of R-DAB with $Os_3(CO)_{12}$, which might have given stable intermediates, owing to the greater Os–Os bond strength, were hindered by the large kinetic stability of $Os_3(CO)_{12}$. Under drastic conditions only the dinuclear $Os_2(CO)_6$(R-DAB(6e)) complexes were isolated in low yield.[7] In order to see whether it was possible to isolate complexes with an intact Os_3 backbone, we turned our attention to reactions of the more reactive trinuclear osmium derivative $Os_3(CO)_{10}(MeCN)_2$ with the α-diimines R-DAB and R-Pyca,[1c] respectively.

In this paper we describe the isolation and characterization of two isomeric triosmium clusters $Os_3(CO)_{10}$(R-DAB), which differ in the mode of bonding of the R-DAB ligand to the $Os_3(CO)_{10}$ unit as well as the fluxional behavior of $Os_3(CO)_{10}$(R-DAB(4e)) in solution.

Experimental Section

Materials and Apparatus. NMR spectra were obtained on Bruker AC100, AC200, and WM250 spetrometers. Variable-temperature NMR experiments were performed on a Bruker AM500 spectrometer. IR spectra were recorded with a Perkin-Elmer 283 spectrometer; low-temperature FTIR spectra were obtained on a Nicolet 7199B FTIR interferometer (liquid-nitrogen-cooled Hg, Cd, Te detector). Field desorption (FD) mass spectra were obtained with a Varian MAT 711 double-focusing mass spectrometer with a combined EI/FD/FI ion source and coupled to a spectrosystem MAT 100 data acquisition unit.[8] Elemental analyses were carried out by the section Elemental Analyses of the Institute of Applied Chemistry, TNO, Zeist, The Netherlands. All preparations were carried out in an atmosphere of purified nitrogen, using carefully dried solvents. The R-DAB (**a**, R = c-Pr; **b**, R = *i*-Pr; **c**, R = neo-Pent; **d**, R = *t*-Bu) ligands have been prepared by the condensation reaction of glyoxal with the appropriate amine.[9a,b] $Os_3(CO)_{12}$ was purchased from Strem Chemicals and used without further purification. $Os_3(CO)_{11}$(MeCN) was prepared by a literature method.[10a] Silica gel (60 mesh) for column chromatography was activated before use.

Synthesis of $Os_3(CO)_{10}(MeCN)_2$. The synthesis of $Os_3(CO)_{10}(MeCN)_2$ was performed by a modified literature procedure.[10b] $Os_3(CO)_{12}$ (1 mmol) was suspended in 100 mL of dry, freshly distilled, MeCN, and the temperature of the solution was raised to just below 50 °C. Oxygen-free N_2 was passed through the solution throughout the reaction. Sublimed Me_3NO (2.1 mmol), dissolved in dry MeCN, was added slowly over a period of 1 h until the bands due to $Os_3(CO)_{12}$ and $Os_3(CO)_{11}(MeCN)$[10a,c] were replaced by those of $Os_3(CO)_{10}(MeCN)_2$.[10b] During the preparation the suspension turned into a bright yellow solution. The solution was then filtered through silica to remove excess of Me_3NO, and the product was isoalted by evaporation of the solvent under vacuum. Typical yields are 90%. IR (CH_2Cl_2, ν(CO), cm^{-1}): 2076, 2026, 2019, 1981, 1960.

Synthesis of $Os_3(CO)_{10}$(R-DAB). The synthesis of all $Os_3(CO)_{10}$(R-DAB) complexes was performed by reaction of $Os_3(CO)_{10}(MeCN)_2$ with R-DAB (**a**, R = c-Pr; **b**, R = *i*-Pr; **c**, R = neo-Pent). For each synthesis basically the same procedure was followed, using either MeCN, THF, or toluene as solvent.

Reactions in MeCN and THF. Synthesis of $Os_3(CO)_{10}$(*i*-Pr-DAB(4e)) (1b), $Os_3(CO)_{10}$(*neo*-Pent-DAB(4e)) (1c), and $Os_3(CO)_{10}$(c-Pr-DAB(6e)) (2a). R-DAB (0.44 mmol) was added to a stirred solution of $Os_3(CO)_{10}(MeCN)_2$ (0.11 mmol), prepared in situ, in MeCN at 45 °C. Alternatively a room-temperature solution of $Os_3(CO)_{10}(MeCN)_2$ in THF was treated with 1 equiv of R-DAB. In both cases the yellow solution turned deep red within a few minutes. After the solution was stirred for 6 h, the solvent was evaporated. The residue was dissolved in 0.5 mL of CH_2Cl_2 and was separated by column chromatography as a red band (eluent hexane/diethyl ether = 10:1). The eluent containing the product was evaporated to 5 mL, and the product precipitated as crystals upon cooling to −80 °C. The mother liquor was decanted, and the crystals were dried in vacuo. With R = *i*-Pr the crystals consisted of **1b** whereas the mother liquor contained a small amount of **2b**. With R = c-Pr a very small amount of dark red crystals, probably $Os_3(CO)_{10}$(c-Pr-DAB(4e)) (**1a**), precipitated together with **2a**, which were removed by washing with 10 mL of cold hexane. The red colored hexane solution obtained by the washings slowly was converted into a solution of yellow **2a**. With R = neo-Pent only **1c** was formed. Yields: red **1b**, 0.03 mmol (30%); red **1c**, 0.03 mmol (30%); yellow **2a**, 0.07 mmol (65%).

Reactions in Toluene. Synthesis of $Os_3(CO)_{10}$(neo-Pent-DAB(4e)) (1c), $Os_3(CO)_{10}$(*i*-Pr-DAB(6e)) (2b), and

(7) Staal, L. H.; van Koten, G.; Vrieze, K. *J. Organomet. Chem.* **1981**, *206*, 99.

(8) Staal, L. H.; van Koten, G.; Fokkens, R. H.; Nibbering, N. M. M. *Inorg. Chim. Acta* **1981**, *50*, 205.

(9) (a) Staal, L. H.; Polm, L. H.; Vrieze, K.; Ploeger, F.; Stam, C. H. *Inorg. Chem.* **1982**, *20*, 3590. (b) Kliegman, J. M.; Barnes, R. K. *J. Org. Chem.* **1970**, *35*, 3140.

(10) (a) Süs-Fink, G. *Z. Naturforsch., B: Anorg. Chem., Org. Chem.* **1980**, *35B*, 454. (b) Tachikawa, M.; Shapley, J. R. *J. Organomet. Chem.* **1977**, *124*, C19. (c) Johnson, B. F. G.; Lewis, J.; Pippard, D. A. *J. Chem. Soc., Dalton Trans.* **1981**, 407.

Table I. Fractional Coordinates of the Atoms and Equivalent Isotropic Thermal Parameters of $Os_3(CO)_{10}$(*i*-Pr-DAB(4e)) (1b)

atom	*x*	*y*	*z*	U_{eq}, Å^2
Os(1)	0.18365 (6)	0.32094 (5)	0.35943 (9)	0.0306 (3)
Os(2)	0.18611 (7)	0.13887 (5)	0.49512 (9)	0.0338 (3)
Os(3)	0.35716 (7)	0.16659 (6)	0.26789 (10)	0.0356 (4)
C(1)	0.099 (3)	0.379 (2)	0.528 (2)	0.055 (12)
C(2)	0.331 (2)	0.377 (1)	0.486 (3)	0.049 (11)
C(3)	0.238 (2)	0.018 (1)	0.568 (3)	0.045 (11)
C(4)	0.096 (2)	0.066 (2)	0.297 (3)	0.048 (11)
C(5)	0.036 (2)	0.164 (2)	0.597 (3)	0.055 (14)
C(6)	0.286 (2)	0.216 (2)	0.674 (3)	0.061 (14)
C(7)	0.416 (2)	0.035 (2)	0.210 (3)	0.058 (14)
C(8)	0.226 (2)	0.155 (2)	0.080 (3)	0.055 (12)
C(9)	0.478 (2)	0.187 (2)	0.466 (3)	0.051 (13)
C(10)	0.464 (2)	0.240 (2)	0.162 (3)	0.057 (14)
C(11)	0.114 (2)	0.390 (2)	0.057 (2)	0.046 (11)
C(12)	0.014 (2)	0.326 (2)	0.069 (2)	0.042 (10)
C(13)	0.304 (2)	0.483 (2)	0.182 (3)	0.046 (11)
C(14)	0.323 (3)	0.500 (3)	0.007 (4)	0.080 (21)
C(15)	0.267 (3)	0.580 (2)	0.287 (3)	0.065 (15)
C(16)	−0.096 (2)	0.233 (2)	0.237 (3)	0.054 (13)
C(17)	−0.171 (2)	0.182 (3)	0.079 (3)	0.071 (17)
C(18)	−0.182 (2)	0.311 (2)	0.319 (3)	0.055 (13)
N(1)	0.203 (2)	0.402 (1)	0.175 (2)	0.039 (8)
N(2)	0.017 (2)	0.287 (1)	0.202 (2)	0.044 (9)
O(1)	0.059 (2)	0.420 (2)	0.641 (2)	0.064 (11)
O(2)	0.418 (2)	0.415 (2)	0.559 (3)	0.076 (13)
O(3)	0.265 (2)	−0.052 (2)	0.619 (3)	0.082 (15)
O(4)	0.046 (2)	0.017 (1)	0.186 (2)	0.060 (10)
O(5)	−0.053 (2)	0.183 (2)	0.662 (2)	0.067 (12)
O(6)	0.342 (2)	0.264 (2)	0.782 (2)	0.075 (13)
O(7)	0.454 (2)	−0.042 (2)	0.167 (3)	0.101 (17)
O(8)	0.160 (1)	0.150 (2)	−0.038 (2)	0.062 (10)
O(9)	0.547 (2)	0.199 (2)	0.572 (3)	0.083 (14)
O(10)	0.530 (2)	0.279 (2)	0.096 (2)	0.067 (12)

$Os_3(CO)_{10}$(c-Pr-DAB(6e)) (2a). R-DAB (0.11 mmol) was added to a stirred yellow suspension of $Os_3(CO)_{10}(MeCN)_2$ (0.11 mmol) in toluene at −20 °C. The suspension was allowed to come to room temperature in about 2 h, during which time the color of the solution turned slowly red. Stirring was continued for another 18 h at 20 °C. The solvent was evaporated, and the residue was dissolved in 0.5 mL of CH_2Cl_2 and was separated by column chromatography as a red band (eluent hexane/diethyl ether = 5:1). The eluent containing the product was evaporated to 5 mL, and the product precipitated as crystals upon cooling to −80 °C. The mother liquor was decanted, and the crystals were dried in vacuo. With R = *i*-Pr the crystals consisted of **2b** whereas the mother liquor contained a small amount of **1b**. With R = c-Pr a very small amount of dark red crystals precipitated together with **2a**, probably **1a** (vide supra). With R = neo-Pent only **1c** was formed. Yields: red **1c**, 0.03 mmol (30%); yellow **2a**, 0.07 mmol (65%); orange **2b**, 0.03 mmol (30%).

All products are extremely soluble in hexane, **2a** being somewhat less soluble.

Attempted Synthesis of $Os_3(CO)_{11}$(*i*-Pr-DAB(2e)). $Os_3(CO)_{11}(MeCN)$ (0.11 mmol) was reacted with *i*-Pr-DAB in 10 mL of acetonitrile, toluene, or benzene, respectively. The reactions were performed by using both 1 and 10 equiv of *i*-Pr-DAB. At room temperature no reaction occurred. At 50 °C in both cases a reaction was observed, but no pure products could be isolated.

Crystal Structure Determination of $Os_3(CO)_{10}$(*i*-Pr-DAB(4e)) (1b; $Os_3C_{18}H_{16}N_2O_{10}$; (3M–M) Decacarbonyl(1,4-diisopropyl-1,4-diaza-1,3-butadiene)triosmium). Crystals of the title compound are triclinic, space group $P\bar{1}$, with two molecules in a unit cell of dimensions a = 10.777 (2) Å, b = 13.562 (2) Å, c = 8.426 (2) Å, α = 98.92 (2)°, β = 96.45 (2)°, and γ = 90.00 (2)°. A total of 6975 independent reflections were measured on a Nonius CAD 4 diffractometer, using graphite monochromated Mo Kα radiation, of which 3026 had intensities below the $3\sigma(I)$ level and were treated as unobserved. The osmium positions were derived from an E^2 Patterson synthesis. A subsequent F_o synthesis revealed the remaining non-hydrogen atoms. After isotropic block-diagonal least-squares refinement, an empirical absorption correction (DIFABS)[11a] was applied (μ(Mo Kα) = 158.1 cm^{-1}).

Table II. Bond Distances of the Atoms (Å) and Standard Deviations in Parentheses of $Os_3(CO)_{10}$(*i*-Pr-DAB(4e)) (1b)

Os(1)–Os(2)	2.876 (2)	C(3)–O(3)	1.13 (2)
Os(1)–Os(3)	2.880 (1)	C(4)–O(4)	1.14 (2)
Os(1)–C(1)	1.85 (2)	C(5)–O(5)	1.17 (2)
Os(1)–C(2)	1.90 (2)	C(6)–O(6)	1.14 (2)
Os(1)–N(1)	2.07 (1)	C(7)–O(7)	1.14 (3)
Os(1)–N(2)	2.11 (1)	C(8)–O(8)	1.15 (2)
Os(2)–Os(3)	2.867 (1)	C(9)–O(9)	1.09 (2)
Os(2)–C(3)	1.90 (1)	C(10)–O(10)	1.13 (2)
Os(2)–C(4)	1.96 (2)	C(11)–C(12)	1.41 (2)
Os(2)–C(5)	1.92 (2)	C(11)–N(1)	1.29 (2)
Os(2)–C(6)	1.92 (2)	C(12)–N(2)	1.31 (2)
Os(3)–C(7)	1.90 (2)	C(13)–C(14)	1.56 (3)
Os(3)–C(8)	1.99 (2)	C(13)–C(15)	1.55 (2)
Os(3)–C(9)	1.98 (2)	C(13)–N(1)	1.54 (2)
Os(3)–C(10)	1.90 (2)	C(16)–C(17)	1.54 (3)
C(1)–O(1)	1.15 (2)	C(16)–C(18)	1.54 (3)
C(2)–O(2)	1.14 (2)	C(16)–N(2)	1.50 (2)

Table III. Bond Angles of the Atoms (deg) with Standard Deviations in Parentheses of $Os_3(CO)_{10}$(*i*-Pr-DAB(4e)) (1b)

Os(2)–Os(1)–Os(3)	59.75 (6)	Os(2)–Os(3)–C(7)	102.4 (8)
Os(2)–Os(1)–C(1)	88.1 (7)	Os(2)–Os(3)–C(8)	94.4 (7)
Os(2)–Os(1)–C(2)	95.8 (6)	Os(2)–Os(3)–C(9)	82.2 (7)
Os(2)–Os(1)–N(1)	153.0 (3)	Os(2)–Os(3)–C(10)	156.0 (5)
Os(2)–Os(1)–N(2)	95.8 (5)	C(7)–Os(3)–C(8)	94 (1)
Os(3)–Os(1)–C(1)	143.4 (6)	C(7)–Os(3)–C(9)	91 (1)
Os(3)–Os(1)–C(2)	80.5 (7)	C(7)–Os(3)–C(10)	100 (1)
Os(3)–Os(1)–N(1)	97.1 (5)	C(8)–Os(3)–C(9)	174.8 (8)
Os(3)–Os(1)–N(2)	106.5 (5)	C(8)–Os(3)–C(10)	91 (1)
C(1)–Os(1)–C(2)	86 (1)	C(9)–Os(3)–C(10)	90 (1)
C(1)–Os(1)–N(1)	117.7 (8)	Os(1)–C(1)–O(1)	172 (1)
C(1)–Os(1)–N(2)	93 (1)	Os(1)–C(2)–O(2)	177 (1)
C(2)–Os(1)–N(1)	93.5 (9)	Os(2)–C(3)–O(3)	176 (1)
C(2)–Os(1)–N(2)	168.3 (7)	Os(2)–C(4)–O(4)	175 (1)
N(1)–Os(1)–N(2)	76.6 (7)	Os(2)–C(5)–O(5)	177 (1)
Os(1)–Os(2)–Os(3)	60.19 (5)	Os(2)–C(6)–O(6)	178 (1)
Os(1)–Os(2)–C(3)	162.6 (4)	Os(3)–C(7)–O(7)	176 (1)
Os(1)–Os(2)–C(4)	91.7 (6)	Os(3)–C(8)–O(8)	173 (1)
Os(1)–Os(2)–C(5)	95.9 (8)	Os(3)–C(9)–O(9)	178 (1)
Os(1)–Os(2)–C(6)	83.9 (9)	Os(3)–C(10)–O(10)	176 (1)
Os(3)–Os(2)–C(3)	103.7 (7)	C(12)–C(11)–N(1)	117 (2)
Os(3)–Os(2)–C(4)	80.0 (6)	C(11)–C(12)–N(2)	117 (2)
Os(3)–Os(2)–C(5)	154.5 (5)	C(14)–C(13)–C(15)	112 (2)
Os(3)–Os(2)–C(6)	93.8 (7)	C(14)–C(13)–N(1)	110 (2)
C(3)–Os(2)–C(4)	91.6 (10)	C(15)–C(13)–N(1)	110 (2)
C(3)–Os(2)–C(5)	101 (1)	C(17)–C(16)–C(18)	107 (2)
C(3)–Os(2)–C(6)	91 (1)	C(17)–C(16)–N(2)	111 (2)
C(4)–Os(2)–C(5)	93 (1)	C(18)–C(16)–N(2)	108 (2)
C(4)–Os(2)–C(6)	173.7 (8)	Os(1)–N(1)–C(11)	116 (1)
C(5)–Os(2)–C(6)	92 (1)	Os(1)–N(1)–C(13)	124.2 (10)
Os(1)–Os(3)–Os(2)	60.06 (5)	C(11)–N(1)–C(13)	120 (2)
Os(1)–Os(3)–C(7)	158.0 (6)	Os(1)–N(2)–C(12)	113 (1)
Os(1)–Os(3)–C(8)	75.7 (6)	Os(1)–N(2)–C(16)	126 (1)
Os(1)–Os(3)–C(9)	99.1 (7)	C(12)–N(2)–C(16)	120 (2)
Os(1)–Os(3)–C(10)	99.2 (8)		

Subsequent anisotropic refinement converged to R = 0.047 and R_w = 0.097 for the 3949 observed reflections. The anomalous dispersion of osmium was taken into account,[11b] and a weighting scheme $\omega = 1/(4.1 + F_o + 0.04F_o^2)$ was applied. The computer programs used were from the XRAY76 system.[11c] The molecular geometry of **1b** with the number of the atoms is given in Figure 1, which shows a PLUTO drawing[11d] of the molecule. Atomic parameters, bond lengths, and bond angles are given in Tables I, II, and III, respectively. A stereo ORTEP drawing, the anisotropic thermal parameters, and a list of observed and calculated structure factors are included in the supplementary material.

(11) (a) Walker, N.; Stuart, D. *Acta Crystallogr., Sect. A: Cryst. Phys., Diffr., Theor. Gen. Crystallogr.* **1983**, *A39*, 158. (b) *International Tables for Crystallography*; Kynoch: Birmingham, 1974; Vol. IV. (c) Stewart, J. M. *The XRay 76 system*; Technical Report TR 446; Computer Science Center, University of Maryland: College Park, MD. (d) Motherwell, S.; Glegg, G. PLUTO, Program for Plotting Molecular and Crystal Structures; University of Cambridge: Cambridge England, 1978.

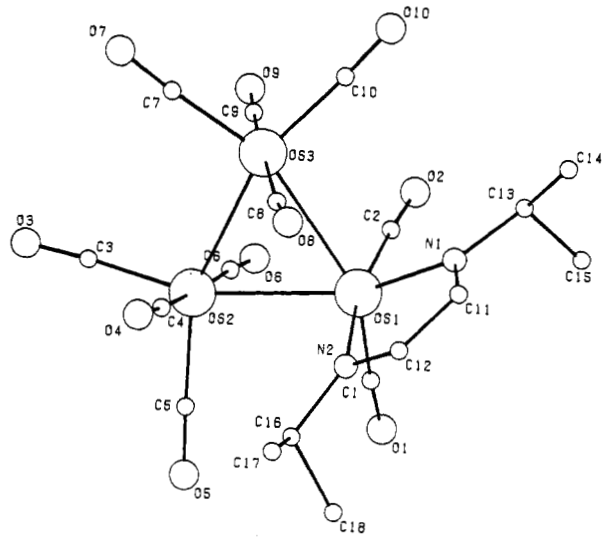

Figure 1. The molecular geometry of $Os_3(CO)_{10}$(*i*-Pr-DAB(4e)) (**1b**).

Table IV. Fractional Coordinates of the Atoms and Equivalent Isotropic Thermal Parameters of $Os_3(CO)_{10}$(c-Pr-DAB(6e)) (2a)

atom	*x*	*y*	*z*	U_{eq}, Å^2
Os(1)	0.20623 (7)	0.14163 (5)	0.35817 (7)	0.0254 (3)
Os(2)	0.45150 (7)	0.33306 (5)	0.61698 (8)	0.0286 (3)
Os(3)	0.20140 (7)	0.25571 (5)	0.68127 (8)	0.0299 (3)
N(1)	0.1280 (15)	0.2736 (12)	0.2994 (16)	0.062 (9)
N(2)	0.3956 (14)	0.2255 (10)	0.3954 (17)	0.057 (8)
O(9)	0.1910 (21)	0.0289 (16)	0.0143 (18)	0.135 (15)
O(10)	0.3500 (17)	−0.0455 (11)	0.4297 (20)	0.100 (12)
O(11)	−0.0773 (15)	0.0528 (13)	0.3480 (19)	0.107 (12)
O(12)	0.7379 (17)	0.4037 (16)	0.5994 (29)	0.146 (18)
O(13)	0.6028 (19)	0.2363 (15)	0.8640 (20)	0.123 (14)
O(14)	0.4101 (21)	0.5411 (12)	0.8428 (22)	0.125 (14)
O(15)	0.3620 (18)	0.0748 (12)	0.7522 (18)	0.103 (12)
O(16)	0.2753 (20)	0.3829 (17)	1.0226 (17)	0.131 (15)
O(17)	−0.0854 (19)	0.1743 (19)	0.6869 (24)	0.153 (18)
O(18)	0.0838 (20)	0.4474 (12)	0.5936 (22)	0.122 (14)
C(1)	0.2210 (17)	0.3469 (14)	0.3202 (22)	0.064 (10)
C(2)	0.3672 (20)	0.3276 (14)	0.3824 (29)	0.082 (14)
C(3)	−0.0185 (18)	0.2884 (15)	0.2425 (21)	0.067 (11)
C(4)	−0.0803 (23)	0.2313 (18)	0.0793 (23)	0.093 (14)
C(5)	−0.0631 (25)	0.3485 (18)	0.1257 (30)	0.101 (17)
C(6)	0.5054 (20)	0.1662 (16)	0.3135 (23)	0.077 (13)
C(7)	0.6170 (24)	0.2202 (22)	0.2627 (31)	0.106 (19)
C(8)	0.5032 (25)	0.1518 (22)	0.1421 (27)	0.102 (18)
C(9)	0.2010 (22)	0.0743 (16)	0.1473 (24)	0.082 (13)
C(10)	0.2957 (19)	0.0274 (13)	0.4056 (21)	0.065 (11)
C(11)	0.0341 (20)	0.0878 (14)	0.3537 (19)	0.064 (11)
C(12)	0.6222 (25)	0.3755 (14)	0.5937 (28)	0.092 (15)
C(13)	0.5391 (21)	0.2736 (15)	0.7691 (25)	0.080 (13)
C(14)	0.4273 (19)	0.4575 (16)	0.7577 (28)	0.084 (14)
C(15)	0.2985 (21)	0.1422 (13)	0.7218 (21)	0.067 (11)
C(16)	0.2460 (22)	0.3346 (15)	0.8880 (21)	0.074 (12)
C(17)	0.0278 (22)	0.2042 (20)	0.6816 (29)	0.097 (17)
C(18)	0.1260 (21)	0.3706 (17)	0.6201 (21)	0.082 (13)

Table V. Bond Distances of the Atoms (Å) with Standard Deviations in Parentheses of $Os_3(CO)_{10}$(c-Pr-DAB(6e)) (2a)

Os(1)–Os(3)	2.931 (3)	N(2)–C(6)	1.50 (2)
Os(1)–N(1)	2.12 (1)	O(9)–C(9)	1.19 (2)
Os(1)–N(2)	2.13 (1)	O(10)–C(10)	1.17 (2)
Os(1)–C(9)	1.88 (2)	O(11)–C(11)	1.19 (2)
Os(1)–C(10)	1.89 (1)	O(12)–C(12)	1.20 (2)
Os(1)–C(11)	1.85 (1)	O(13)–C(13)	1.21 (2)
Os(2)–Os(3)	2.928 (5)	O(14)–C(14)	1.21 (2)
Os(2)–N(2)	2.12 (1)	O(15)–C(15)	1.17 (2)
Os(2)–C(2)	2.14 (2)	O(16)–C(16)	1.20 (2)
Os(2)–C(12)	1.86 (2)	O(17)–C(17)	1.21 (2)
Os(2)–C(13)	1.88 (2)	O(18)–C(18)	1.19 (2)
Os(2)–C(14)	1.85 (2)	C(1)–C(2)	1.48 (2)
Os(3)–C(15)	1.89 (1)	C(3)–C(4)	1.49 (2)
Os(3)–C(16)	1.87 (1)	C(3)–C(5)	1.54 (2)
Os(3)–C(17)	1.86 (2)	C(4)–C(5)	1.54 (3)
Os(3)–C(18)	1.91 (2)	C(6)–C(7)	1.55 (2)
N(1)–C(1)	1.33 (2)	C(6)–C(8)	1.53 (2)
N(1)–C(3)	1.46 (2)	C(7)–C(8)	1.53 (3)
N(2)–C(2)	1.45 (2)		

Table VI. Bond Angles of the Atoms (deg) with Standard Deviations in Parentheses of $Os_3(CO)_{10}$(c-Pr-DAB(6e)) (2a)

Os(3)–Os(1)–N(1)	87.5 (4)	C(15)–Os(3)–C(16)	92.5 (9)
Os(3)–Os(1)–N(2)	84.4 (4)	C(15)–Os(3)–C(17)	94 (1)
Os(3)–Os(1)–C(9)	176.4 (5)	C(15)–Os(3)–C(18)	170.5 (7)
Os(3)–Os(1)–C(10)	94.5 (6)	C(16)–Os(3)–C(17)	99 (1)
Os(3)–Os(1)–C(11)	86.5 (5)	C(16)–Os(3)–C(18)	91.6 (9)
N(1)–Os(1)–N(2)	79.6 (6)	C(17)–Os(3)–C(18)	94 (1)
N(1)–Os(1)–C(9)	89.2 (8)	Os(1)–N(1)–C(1)	116 (1)
N(1)–Os(1)–C(10)	173.4 (6)	Os(1)–N(1)–C(3)	124.3 (10)
N(1)–Os(1)–C(11)	95.8 (8)	C(1)–N(1)–C(3)	120 (1)
N(2)–Os(1)–C(9)	96.3 (8)	Os(1)–N(2)–Os(2)	115.3 (5)
N(2)–Os(1)–C(10)	94.3 (7)	Os(1)–N(2)–C(2)	111 (1)
N(2)–Os(1)–C(11)	169.9 (6)	Os(1)–N(2)–C(6)	114.3 (10)
C(9)–Os(1)–C(10)	89.0 (9)	Os(2)–N(2)–C(2)	71 (1)
C(9)–Os(1)–C(11)	92.5 (9)	Os(2)–N(2)–C(6)	120.6 (9)
C(10)–Os(1)–C(11)	90.6 (9)	C(2)–N(2)–C(6)	118 (1)
Os(3)–Os(2)–N(2)	84.7 (4)	N(1)–C(1)–C(2)	117 (1)
Os(3)–Os(2)–C(2)	96.7 (6)	Os(2)–C(2)–N(2)	69 (1)
Os(3)–Os(2)–C(12)	173.1 (6)	Os(2)–C(2)–C(1)	126 (1)
Os(3)–Os(2)–C(13)	81.8 (7)	N(2)–C(2)–C(1)	116 (1)
Os(3)–Os(2)–C(14)	88.7 (7)	N(1)–C(3)–C(4)	118 (1)
N(2)–Os(2)–C(2)	39.9 (6)	N(1)–C(3)–C(5)	121 (1)
N(2)–Os(2)–C(12)	98.0 (8)	C(4)–C(3)–C(5)	61 (2)
N(2)–Os(2)–C(13)	113.1 (8)	C(3)–C(4)–C(5)	61 (2)
N(2)–Os(2)–C(14)	150.4 (7)	C(3)–C(5)–C(4)	58 (2)
C(2)–Os(2)–C(12)	89.4 (9)	N(2)–C(6)–C(7)	122 (1)
C(2)–Os(2)–C(13)	152.6 (7)	N(2)–C(6)–C(8)	122 (1)
C(2)–Os(2)–C(14)	113.1 (10)	C(7)–C(6)–C(8)	59 (2)
C(12)–Os(2)–C(13)	91 (1)	C(6)–C(7)–C(8)	59 (2)
C(12)–Os(2)–C(14)	92 (1)	C(6)–C(8)–C(7)	61 (2)
C(13)–Os(2)–C(14)	94 (1)	Os(1)–C(9)–O(9)	176 (1)
Os(1)–Os(3)–Os(2)	75.6 (1)	Os(1)–C(10)–O(10)	178 (1)
Os(1)–Os(3)–C(15)	83.5 (6)	Os(1)–C(11)–O(11)	179 (1)
Os(1)–Os(3)–C(16)	165.4 (4)	Os(2)–C(12)–O(12)	171 (1)
Os(1)–Os(3)–C(17)	95.0 (8)	Os(2)–C(13)–O(13)	176 (1)
Os(1)–Os(3)–C(18)	90.5 (6)	Os(2)–C(14)–O(14)	176 (1)
Os(2)–Os(3)–C(15)	91.2 (7)	Os(3)–C(15)–O(15)	177 (1)
Os(2)–Os(3)–C(16)	90.5 (7)	Os(3)–C(16)–O(16)	178 (1)
Os(2)–Os(3)–C(17)	168.7 (5)	Os(3)–C(17)–O(17)	177 (1)
Os(2)–Os(3)–C(18)	80.1 (7)	Os(3)–C(18)–O(18)	175 (1)

Crystal Structure Determination of $Os_3(CO)_{10}$(c-Pr-DAB(6e)) (2a; $Os_3C_{18}H_{12}N_2O_{10}$; (2M–M) Decacarbonyl(1,4-dicyclopropyl-1,4-diaza-1,3-butadiene)triosmium). Crystals of **2a** are triclinic, space group $P\bar{1}$, with two molecules in a unit cell of dimensions a = 9.775 (3) Å, b = 13.730 (4) Å, c = 9.222 (5) Å, α = 107.39 (3)°, β = 101.04 (5)°, and γ = 87.84 (3)°. A total of 6692 independent reflections were measured on a Nonius CAD 4 diffractometer, using graphite-monochromated Mo Kα radiation, of which 2449 had intensities below the 2.5$\sigma(I)$ level and were treated as unobserved. The osmium positions were derived from an E^2 Patterson synthesis. A subsequent F_o synthesis revealed the remaining non-hydrogen atoms. After isotropic block-diagonal least-squares refinement an empirical absorption correction (DIFABS)[11a] was applied (μ(Mo Kα) = 164.8 cm^{-1}). Subsequent anisotropic refinement converted to R = 0.052 and R_w = 0.059 for the 4243 observed reflections. The anomalous dispersion of osmium was taken into account,[11b] and unit weights were applied. The computer programs used were from the XRAY76 system.[11c] The molecular geometry of **2a** with the numbering of the atoms is given in Figure 2, which shows a PLUTO drawing[11d] of the molecule. Atomic parameters, bond lengths, and bond angles are given in Tables IV, V, and VI, respectively. A stereo ORTEP drawing, the anisotropic thermal parameters, and a list of observed and calculated structure factors are included in the supplementary material.

Analytical Data. Elemental analysis of all complexes gave satisfactory results (see supplementary material). The IR data are listed in Table VII. The osmium carbonyl R-DAB clusters

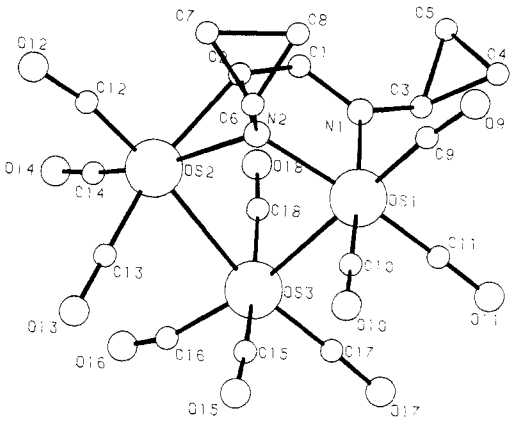

Figure 2. The molecular geometry of $Os_3(CO)_{10}$(c-Pr-DAB(6e)) (**2a**).

Table VII. IR and FD Mass Spectral Data

compound	m/z(obsd)[a]	IR ν(CO),[b] cm^{-1}
$Os_3(CO)_{10}$(*i*-Pr-DAB(4e)) (**1b**)	994 (992)	2092, 2046, 2020, 2004, 1994, 1979, 1964, 1921
$Os_3(CO)_{10}$(neo-Pent-DAB(4e)) (**1c**)	1052 (1048)	2099, 2053, 2024, 2013, 1999, 1982, 1964, 1917
$Os_3(CO)_{10}$(c-Pr-DAB(6e)) (**2a**)	989 (988)	2087, 2052, 2027, 2008, 1992, 1985, 1976, 1970, 1957
$Os_3(CO)_{10}$(*i*-Pr-DAB(6e)) (**2b**)	991 (992)	2087, 2050, 2028, 2008, 1991, 1983, 1976, 1970, 1955

[a] Calculated values in parentheses. The measured and calculated values account for the highest peak in the measured and simulated isotope patterns. [b] In hexane.

show characteristic absorption patterns in the terminal ν(CO) region. Within a group of one type of isomer the spectra are similar. The spectra of isomers 1 and 2 differ in the 1900–1975 cm^{-1} region: isomers 1 show characteristic absorptions at 1921 and 1964 cm^{-1} while isomers 2 absorb at 1955 and 1970 cm^{-1}. For complexes **1b** and **1c** IR spectra were recorded of the solids in KBr and in pentane solution at 148 K. These spectra were found to be identical with those of the solutions at room temperature; see Table VII. This is an indication that the structures in solution and in the solid state are similar. FD mass spectra were recorded by using the field desorption technique. The spectra show an Os_3 isotopic pattern around the m/z value of the molecule ion that agreed with the simulated spectra; see Table VII. No peaks due to the $[M - CO]^+$ species were observed.

Results and Discussion

Formation of Products. Schematic structures of the products are depicted in Figure 3.

Reaction Conditions. The reactions of $Os_3(CO)_{10}(MeCN)_2$ with R-DAB were carried out in MeCN, THF, or toluene. When the reactions were performed in MeCN, an excess of ligand was needed for the reaction to take place, whereas the reactions in THF and toluene could be performed by employing 1 equiv of ligand. The reactions in MeCN were slow at 20 °C and were best performed at 45 °C. The reactions in THF and toluene were performed at room temperature. However, when started at room temperature, the reactions in toluene were accompanied by extensive decomposition. Higher yields were obtained when these reactions were started at −20 °C. We may conclude that for the reaction in MeCN the excess of MeCN is the cause of the low reactivity with only 1 equiv of R-DAB.

Product Distribution. The formation of products depended on the R group of the R-DAB ligand and in the case of R = *i*-Pr also on the solvent. With R = *t*-Bu as substituent no reaction occurred in either solvent. When refluxing toluene was employed, only decomposition was observed. In the case of R = neo-Pent only **1c** was formed irrespective of whether the reactions were carried out in MeCN, THF, or toluene. A similar effect was observed for R = c-Pr; independent of the solvent only **2a** was the product. For R = *i*-Pr the reaction may proceed via two pathways. Which pathway is chosen depends delicately on the polarity of the solvents, since the reaction in MeCN and THF gave **1b**, whereas in toluene **2b** was formed. In both cases the product that was eluted by chromatography contained very little of the other isomer as was evidenced by ^{1}H NMR and IR spectroscopy.

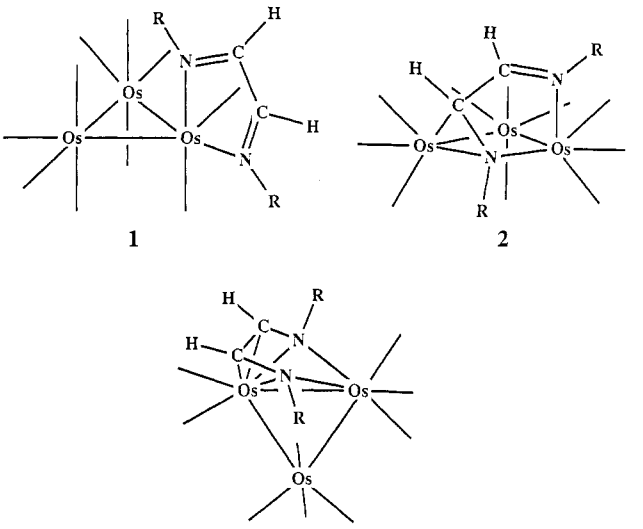

Figure 3. Schematic structures of the complexes $Os_3(CO)_{10}$(R-DAB(4e)) (**1b**, R = *i*-Pr; **1c**, R = neo-Pent), $Os_3(CO)_{10}$(R-DAB(6e)) (**2a**, R = c-Pr; **2b**, R = *i*-Pr), and $Os_3(CO)_9$(R-DAB(8e)) (**3a**, R = c-Pr; **3b**, R = *i*-Pr).

Stability of Complexes. At room temperature all complexes are stable in solution, except for a red byproduct isolated in very small yield in the reaction of c-Pr-DAB with $Os_3(CO)_{10}(MeCN)_2$ which is probably **1a**. The latter compound converted slowly at room temperature into **2a**. The conversion of **2a** into $Os_3(CO)_9$(c-Pr-DAB(8e)) (**3a**), the comparable conversion of **1b** via **2b** to $Os_3(CO)_9$(*i*-Pr-DAB(8e)) (**3b**), and the crystallographic details of the unusual compound **3b** will be the subject of a forthcoming publication.[12]

Molecular Geometry of $Os_3(CO)_{10}$(*i*-Pr-DAB(4e)) (1b). The molecualr geometry of **1b** together with the atomic numbering is given in Figure 1. In Tables II and III the bond lengths and angles are given.

The molecular structure of **1b** is as one would expect for a trinuclear 48e cluster. The molecule contains a triangular array of osmium atoms, two of which, Os(2) and Os(3), are linked to four terminal carbonyl ligands and one of which, Os(1), is linked to two carbonyl ligands and two nitrogen atoms of the chelating R-DAB ligand. One of the nitrogen atoms of the latter ligand is axially and the other equatorially bonded to Os(1) [Os(1)–N = 2.09 (1) Å (mean)]. The 48e cluster **1b** is with respect to the Os_3 unit structurally related to $Os_3(CO)_{12}$ with similar Os–Os bond lengths. For **1b** 2.875 (1) Å (mean) compared to 2.8771 (27) Å (mean) for $Os_3(CO)_{12}$.[13]

(12) Part 2: Zoet, R.; van Koten, G.; Stam, C. H.; Stufkens, D. J.; Vrieze, K. *Organometallics*, following paper in this issue.
(13) Churchill, M. R.; DeBoer, B. G. *Inorg. Chem.* **1977**, *16*, 878.

When carbonyls are substituted for nitrogen-containing ligands, two effects are commonly observed with respect to the carbonyls: first, shortening of the M–C(O) bond lengths and, second, a tendency for bridging of some of the remaining carbonyls. First, both the equatorial and axial CO ligands bonded to Os(1) experience greater π-back-bonding from osmium and are associated with shorter Os–C bonds: Os(1)–C(1)(equatorial) = 1.85 (2) Å [other equatorial CO ligands Os(2)–C(3) = 1.90 (1), Os(2)–C(5) = 1.92 (2), Os(3)–C(7) = 1.90 (2), Os(3)–C(10) = 1.90 (2) Å] and Os(1)–C(2)(axial) = 1.90 (2) Å [other axial CO ligands Os(2)–C(4) = 1.96 (2), Os(2)–C(6) = 1.92 (2), Os(3)–C(8) = 1.99 (2), Os(3)–C(9) = 1.98 (2) Å]. The Os(1)–C(1) equatorial bond is shorter than the Os(1)–C(2) axial bond. A similar effect is found in $[HOs_3(CO)_{10}(MeC{=}CHCOMe)]$[14] and $[HOs_3(CO)_9(C_{10}H_7N_2)]$.[15] Also Os(2)–C(6)(axial) [1.92 (2) Å] is shortened probably due to the influence of N(2). Second, the axial CO ligands show a tendency for taking semibridging positions instead of terminal positions, as in $Os_3(CO)_{12}$, and are leaning toward neighboring metals as indicated by rather acute angles [Os(3)–Os(1)–C(2) = 80.5 (7)°, Os(3)–Os(2)–C(4) = 80.0 (6)°, Os(1)–Os(2)–C(6) = 83.9 (9)°, Os(1)–Os(3)–C(8) = 75.7 (6)°, Os(2)–Os(3)–C(9) = 82.2 (7)°]. In particular the Os(1)–Os(3)–C(8) angle is acute and the C(8)O(8) carbonyl can be considered to be in a semibridging position toward Os(1).[16] In the related cluster $[Ru_3(CO)_{10}(bpy)]$[17] two bridging carbonyl groups are found. However, R-DAB is a better π-acceptor then the bipyridine ligand while, moreover, carbonyl ligands generally appear to prefer terminal positions in complexes of third-row elements, so no symmetrically bridging carbonyls are found in **1b**.

Compared to the free c-Hex-DAB ligand the C=N bonds in **1b** are slightly elongated whereas the central C(11)–C(12) bond is slightly shortened [**1b**, C(11)–N(1) = 1.29 (2) Å, C(12)–N(2) = 1.31 (2) Å, and C(11)–C(12) = 1.41 (2) Å; free ligand, C=N = 1.258 (3) Å, C—C′ = 1.457 (3) Å].[18] The values of **1b** are in the same range as are found in $ReCl(CO)_3$(*i*-Pr-DAB(4e)) [C=N = 1.31(2) Å (mean) and C—C′ = 1.38 (5) Å].[19]

The chelating σ,σ-N,N′ bonded diimine displays a characteristic bite angle at the metal center of 76.6 (7)° which is comparable to that of 72.7 (7)° observed in $[ReCl(CO)_3$(*i*-Pr-DAB(4e))]. The plane defined by Os(1), N(1), C(11), C(12), N(2) is almost perfectly flat, the largest deviation being N(2), which is 0.03 Å out of the least-squares plane.

Molecular Geometry of $Os_3(CO)_{10}$(c-Pr-DAB(6e)) (2a). The molecular geometry of **2a** together with the atomic numbering is given in Figure 2. In Tables V and VI the bond lengths and angles are given.

The R-DAB ligand acts as a 6e donor: σ-N to Os(1) [Os(1)–N(1) = 2.12 (1) Å], symmetrically μ_2-N′ bridging Os(1) and Os(2) [Os(1)–N(2) = 2.13 (1) Å and Os(2)–N(2) = 2.12 (1) Å], and η^2-C=N′ to Os(2) by means of the imine π-C=N bond [Os(2)–C(2) = 2.14 (2) Å and Os(2)–N(2) = 2.12 (1) Å]. The fact that the bonding of the c-Pr-DAB ligand to the $Os_3(CO)_{10}$ unit also comprises the additional electron pair from the π-C=N bond makes **2a** a 50e system. As compared to the 48e system of **1b**, the 50e system of **2a** involves the rupture of the Os(1)–Os(2) bond and consequently the opening of the metal triangle [Os(1)–Os(3)–Os(2) = 75.6 (1)°].[20]

The carbonyl distribution is the same as found in the starting complex $Os_3(CO)_{10}(MeCN)_2$.[21] Os(3) is linked to four terminal carbonyl ligands, and Os(1) and Os(3) are each linked to three terminal carbonyl ligands. All osmium atoms are approximately octahedrally coordinated.

The molecular structure of this second isomer is novel, since it is the first example of a trinuclear compound containing a 6e-donating R-DAB ligand bridging a nonbonded metal pair [Os(1)···Os(2) = 3.591 (3) Å]. The Os(1)–Os(3) and Os(2)–Os(3) bonds have normal single bond lengths of 2.931 (3) and 2.928 (5) Å, respectively.

The NCCN skeleton is virtually flat, while the N(2)–C(6) bond is out of the plane defined by the NCCN skeleton. The bond lengths in the NCCN skeleton are as one would expect for a 6e-donating R-DAB ligand. The σ-N-coordinated imine bond C(1)–N(1) in **2a** has a bond length of 1.33 (2) Å. This length can be compared to that of 1.258 (3) Å in the free *c*-Hex-DAB ligand.[18] The coordinated imine bond C(2)–N(2) is elongated to 1.45 (2) Å, which is close to the single C–N bond length. The C=N bond lengthening is due to the π-back-bonding from Os(2) into the LUMO of the diimine, which is antibonding between C and N. In other complexes with an R-DAB ligand in the 6e coordination mode also a lengthening of the coordinated imine bond is observed; e.g., the η^2-C(H)=N bonded moiety in $Ru_2(CO)_4$(R-DAB(6e))$_2$ is 1.43 (1) Å.[22] The central C(1)–C(2) distance of 1.48 (2) Å is normal for a single carbon–carbon (sp^2–sp^2) bond and similar to that of 1.457 (3) Å in free *c*-Hex-DAB. This is unexpected since the LUMO of the diimine is bonding between C(1) and C(2). For example, in **1b** the central C(11)–C(12) is shortened to 1.41 (2) Å.

It should be noted here that complexes with a 6e-donor R-DAB ligand bridging two metals with a metal–metal bond are quite common.[7,22-24] However, it is clear that 6e-donor R-DAB ligands are also capable of bridging much larger distances between metal atoms, which until now has been found only for $Ru_2(CO)_4$(R-DAB(6e))$_2$. The crystal structure determination of $Ru_2(CO)_4$(R-DAB(6e))$_2$ shows a nonbonding Ru···Ru distance of 3.308 (1) Å; the two nitrogen atoms bridging the two metals [Ru–N = 2.13 (1)

(14) Deeming, A. J.; Manning, P. J.; Rothwell, I. P.; Hurthouse, M. B.; Walker, N. P. C. *J. Chem. Soc., Dalton Trans.* **1984**, 2039.

(15) Deeming, A. J.; Peters, R.; Hursthouse, M. B.; Backer-Dirks, J. D. J. *J. Chem. Soc., Dalton Trans.* **1982**, 787.

(16) In consideration of "semibridging" carbonyl groups, it is customary to calculate the α-value, defined as $(d_2 - d_1)/d_1$ (where d_1 and d_2 are the shorter and longer M–CO distances, respectively). Values with α between 0.1 and 0.6 are considered as "semibridging". Yeh, W.-Y.; Shapley, J. R.; Li, Y.-J.; Churchill, M. R. *Organometallics* **1985**, *4*, 767. Comparison of Os(3)–C(8) and Os(1)–C(8) distances in the present molecule yields an equivalent α-value of 0.54 (i.e. (3.07–1.99)/1.99), which falls near the weak interaction end of the semibridging region.

(17) Venalainen, T.; Pursiainen, J.; Pakkanen, T. A. *J. Chem. Soc., Chem. Commun.* **1985**, 1348.

(18) Vrieze, K.; van Koten, G.; Keijsper, J.; Stam, C. H. *Polyhedron* **1983**, *2*, 1111.

(19) Graham, A. J.; Akrigg, D.; Sheldrick, B. *Cryst. Struct. Commun.* **1977**, *6*, 577.

(20) Other examples of trinuclear osmium clusters with two metal–metal bonds and bridging ligands are $[PPN][Os_3(CO)_{10}(\mu\text{-}CH_2)(\mu\text{-}I)]$, with Os···Os = 3.112 (1) Å: Geoffroy, G. L.; Morrison, E. D. *Organometallics* **1985**, *4*, 1413. $Os_3(CO)_{10}(C(CH_2))_2$ with Os···Os = 3.860 Å: Lewis, J.; Johnson, B. F. G.; Raithby, P. R.; Sankey, S. W. *J. Organomet. Chem.* **1982**, *231*, C65. $Os_3(CO)_{10}(MeO_2CN{=}NCO_2Me)$ with Os···Os = 4.1615 (1) Å: Einstein, W. F. B.; Nussbaum, S.; Sutton, D.; Willis, A. C. *Organometallics* **1984**, *3*, 568. When there are no bridging ligands, approximately linear structures are found, e.g., $HOs_3(CO)_{10}(PEt_3)(CF_3CCHCF_3)$: Mays, M. J.; Raithby, P. R.; Dawoodi, Z. *J. Chem. Soc., Chem. Commun.* **1979**, 721. $HOs_3(CO)_{10}(NC_5H_4CH{=}CH)$: Deeming, A. J.; Burgess, K.; Holden, H. D.; Lewis, J.; Johnson, B. F. G. *J. Chem. Soc., Dalton Trans.* **1985**, 85.

(21) Dawson, P. A.; Puga, J.; Raithby, J. R.; Rosales, J.; Lewis, J.; Johnson, B. F. G. *J. Chem. Soc., Dalton Trans.* **1982**, 233.

(22) Staal, L. H.; Polm, L. H.; Balk, R. W.; van Koten, G.; Vrieze, K.; Brouwers, A. M. F. *Inorg. Chem.* **1980**, *19*, 3343.

(23) Frühauf, H. W.; Landers, A.; Goddard, R.; Krüger, C. *Angew. Chem.* **1978**, *90*, 56.

(24) Staal, L. H.; Keijsper, J.; van Koten, G.; Vrieze, K.; Cras, J. A.; Bosman, W. P. *Inorg. Chem.* **1981**, *20*, 555.

Table VIII. ^{1}H NMR[a] Data

compound	R group	imine H
$Os_3(CO)_{10}$(*i*-Pr-DAB(4e))[b] (**1b**)	1.02 (d, 6 Hz, 6 H)/ 1.08 (d, 6 Hz, 6 H) 4.58 (sept, 6 Hz, 2 H)	7.74 (s, 2 H)
$Os_3(CO)_{10}$(*i*-Pr-DAB(4e))[c] (**1b**)	1.30 (d, 6 Hz, 6 H)/ 1.33 (d, 6 Hz, 6 H) 4.54 (sept, 6 Hz, 2 H)	8.41 (s, 2 H)
$Os_3(CO)_{10}$(neo-Pent-DAB(4e))[b] (**1c**)	0.81 (s, 18 H) 3.53 (d, 12 Hz, 2 H)/ 4.10 (d, 12 Hz, 2 H)	7.36 (s, 2 H)
$Os_3(CO)_{10}$(neo-Pent-DAB(4e))[c] (**1c**)	0.88 (s, 18 H) 3.78 (d, 12 Hz, 2 H)/ 3.90 (d, 12 Hz, 2 H)	7.86 (s, 2 H)
$Os_3(CO)_{10}$(c-Pr-DAB(6e))[b] (**2a**)	0.31 (m, 1 H); 0.53 (m, 1 H); 0.71 (m, 1 H) 0.75 (d, 2 H); 1.04 (d, 2 H); 1.17 (m, 1 H) 2.88 (m, 1 H); 3.44 (m, 1 H)	3.46 (d, 1 Hz, 1 H) 8.34 (d, 1 Hz, 1 H)
$Os_3(CO)_{10}$(*i*-Pr-DAB(6e))[b] (**2b**)	0.57 (d, 7 Hz, 3 H)/ 0.80 (d, 7 Hz, 3 H) 0.92 (d, 7 Hz, 3 H)/ 1.11 (d, 7 Hz, 3 H) 1.44 (sept, 7 Hz, 1 H); 3.30 (sept, 7 Hz, 1 H)	3.02 (d, 1 Hz, 1 H) 7.50 (d, 1 Hz, 1 H)

[a] Shifts are in ppm relative to TMS; vertical bars separate diastereotopic pairs; Abbreviations: d, doublet; s, singlet; m, multiplet; sept, septet. [b] In benzene-d_6, 250 MHz, 293 K. [c] In dichloromethane-d_2, 500 MHz, 193 K.

Table IX. ^{13}C NMR[a] Data

compound	R group	imine C	carbonyls
$Os_3(CO)_{10}$(*i*-Pr-DAB(4e))[b] (**1b**)	21.3/27.0; 65.4	144.4	169.8; 174.3; 182.9; 184.0; 188.2
$Os_3(CO)_{10}$(neo-Pent-DAB(4e))[b] (**1c**)	27.0; 32.7; 75.9	146.1	168.6; 173.3; 183.1; 184.0; 189.6
$Os_3(CO)_{10}$(c-Pr-DAB(6e))[c] (**2a**)	7.7/8.2; 8.4/11.3; 45.4; 47.8	179.6; 59.8	166.5; 172.9; 178.0; 179.6; 181.3; 181.9; 182.5; 184.4; 185.6; 186.3

[a] In dichloromethane-d_2. Shifts are in ppm relative to TMS; vertical bars separate diastereotopic pairs. [b] 125.77 MHz, 193 K. [c] 62.5 MHz, 293 K. Recorded by using an attached proton test pulse sequence.

Å (mean)] with a Ru–(μ-N)–Ru angle of 101.3 (2)°. The Os–N distances in **2a** are in the same range, but the nonbonding Os···Os distance of 3.591 (3) Å is significantly longer then the Ru···Ru distance in the $Ru_2(CO)_4$(R-DAB(6e))$_2$ complex. As a result of this the Os(1)–N(2)–Os(2) angle has also further opened to 115.3 (5)°.

Owing to the back-bonding interaction between Os(2) and C(2)N(2), N(2) has acquired a pseudotetrahedral configuration pointing to a sp^3-hybridized N(2) center. The angles around N(2) are close to those expected for a tetrahedral environment, with the exception of the acute C(2)–N(2)–Os(2) angle of 71 (1)° which is a consequence of the C(2)–Os(2) interaction. Accordingly the Os(1)–N(2) and Os(2)–N(2) bonds are best viewed as covalent 2e–2c bonds.

NMR Spectroscopy. The ^{1}H and ^{13}C NMR data are listed in Tables VIII and IX, respectively.

Complexes 2a and 2b. The ^{1}H NMR data for **2a** (R = c-Pr) and **2b** (R = *i*-Pr) at 300 K show an AX pattern for the imine protons, and two separate resonances are found for the imine carbon atoms of **2b**. The imine proton and carbon atom belonging to the η^2-C(H)=N bonded moiety of the R-DAB ligand shows a characteristic upfield shift and absorb at about 3 and 59.8 ppm, respectively.

Scheme II. Proposed Mechanism of Exchange in the Temperature Range 193–273 K

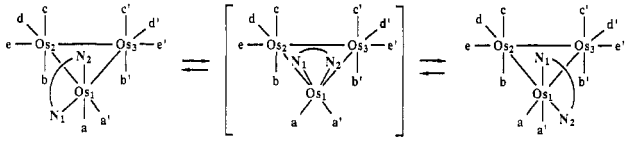

The imine proton and carbon atom of the σ-N=C(H) bonded part absorb around 8 and 179.6 ppm, respectively, which is close to the value normally observed for σ,σ-N,N′ bonded R-DAB groups.[2,9a,22,24] The R groups of the two halves of the R-DAB ligands are magnetically inequivalent and give rise to separate absorptions which is in accordance with the solid-state structure of **2a**.

Complexes 1b and 1c. The ^{1}H and ^{13}C NMR spectra of the isomers **1b** and **1c** do not show a clear-cut one to one correspondence with the solid-state structure of **1b** which has C_1 symmetry. The ^{1}H NMR spectra for **1b** and **1c** between 193 and 308 K show for the two imine protons one sharp signal around 7.5 ppm, while the R substituents are magnetically equivalent, although for **1b** the *i*-Pr methyls and for **1c** the neo-Pent CH_2 are diastereotopic (see Table VIII). The same accounts for the ^{13}C NMR spectra between 193 and 308 K. For both **1b** and **1c** a single carbon resonance is observed at 145 ppm for the two imine carbons. For **1c** single resonances are observed for both neo-Pent groups while for complex **1b** a single resonance is observed for the two methine carbons and two resonances which can be assigned to two diastereotopic isopropyl methyl groups.

On first sight this seems not in accord with the axial–equatorial mode of bonding of the σ,σ-N,N′ chelating *i*-Pr-DAB of **1b** in the solid state (Figure 1). In the ^{1}H NMR of **1b** and **1c** this would give rise to an AX pattern for the imine protons. The *i*-Pr groups in **1b** would give four doublets and two septets. The neo-Pent groups in **1c** would give rise to two singlets for the methyls and two AB patterns for the CH_2 part of the ligand. Also in the ^{13}C NMR the two halves of the ligand would be inequivalent and give rise to separate signals. Likewise at 193 K for the ^{13}C (carbonyl) resonances five ^{13}CO signals are observed for **1c** at 189.6, 183.1, 177.3, 168.6, and 161.1 ppm (together with some small not well-resolved resonances) of relative intensity 1:1:1:1:1. Also five signals were observed in the case of **1b** at 188.2, 184.0, 182.9, 174.3, and 169.8 ppm at 193 K of relative intensity 1:1:1:1:1 (Figure 4). In theory we would have expected ten ^{13}CO signals for the ten inequivalent CO groups or at least nine as in the case of the isostructural $Os_3(CO)_{10}(\eta^4$-cyclohexa-1,3-diene).[25]

These observations indicate that compounds **1b** and **1c** are involved in fluxional processes, which is not surprising, since such processes are well-known for analogous compounds, e.g. $Os_3(CO)_{10}(\eta^4$-cyclohexa-1,3-diene), $Os_3(CO)_{10}$(1,1-$PMe_2Ph)_2$,[26] and $Os_3(CO)_{10}$(1,1-$Ph_2P(CH_2)_2PPh_2$).[27] For reasons that will become clear in the course of this discussion the five ^{13}C signals of the CO ligands of **1b** and **1c** are assigned as shown in Table X, in which also signals of published compounds are listed. We will further restrict the discussion to **1b**, for which the best spectra were obtained and for which the structure in the solid state is known unambiguously.

(25) Bryan, E. G.; Johnson, B. F. G.; Lewis, J. *J. Chem. Soc., Dalton Trans.* **1977**, 144.
(26) Deeming, A. J.; Donovan-Mtunzi, S.; Kabir, S. E.; Manning, P. J. *J. Chem. Soc., Dalton Trans.* **1985**, 1037.
(27) Deeming, A. J.; Donovan-Mtunzi, S.; Kabir, S. E. *J. Organomet. Chem.* **1984**, *276*, C65.

Table X. ^{13}C(Carbonyl) NMR Data (ppm) of Reported Compounds and of $Os_3(CO)_{10}$(*i*-Pr-DAB(4e)) (1b)

compound	aa′	bb′	cc′	dd′	ee′[a]	temp (K)	ref
$Os_3(CO)_{10}$(*i*-Pr-DAB(4e)) (**1b**)	188.2	184.0	182.9	169.8	174.3	193	
$Os_3(CO)_{10}$(cyclohexadiene)[b]	181.8	185.6	184.4	168.9	174.5	233	25
$Os_3(CO)_{10}(1,1\text{-}Ph_2P(CH_2)PPh_2)$[c]	197.9	185.8		178.2	170.9	293	27
$Os_3(CO)_{10}(1,1\text{-}PMe_2Ph)_2$[c,d]	202.1	186.7		179.4	170.3	243	26

[a] Indices are as in Scheme II. [b] The diene ligand is in an axial–equatorial position. [c] The phosphorus atoms are in equatorial positions; thus bb′ = cc′. [d] The relative assignment of dd′ and ee′ were only made tentatively on basis of the dynamic behavior observed in the reported spectra above 243 K. A similar assignment for **1b** would involve a pairwise bridge–terminal exchange in the bb′cc′ee′ plane which would not only leave the dd′ peak sharp but also the aa′ peak. However, this is not the case since for temperatures above 203 K aa′ exchanges clearly with bb′, cc′, and dd′ (see text).

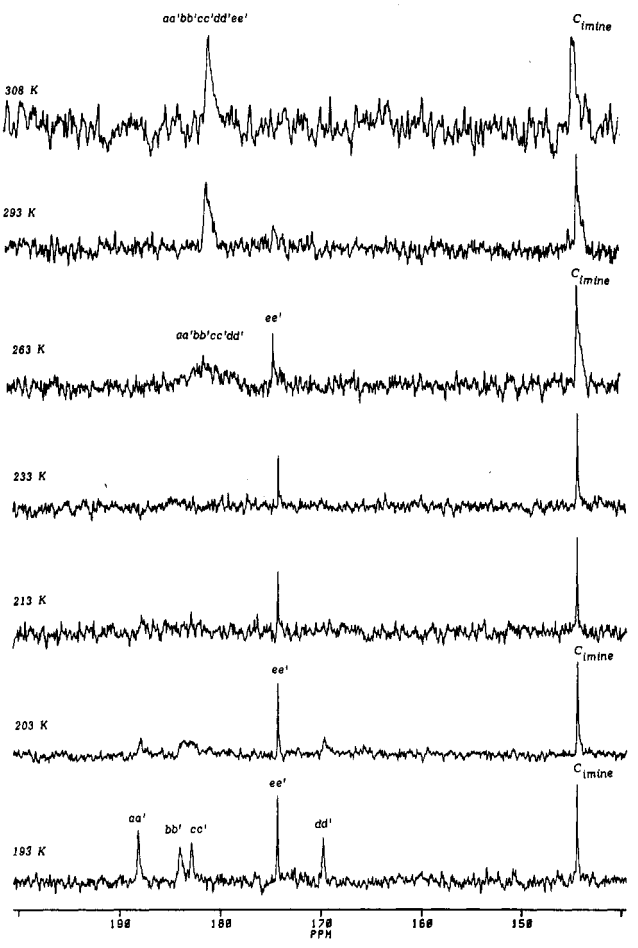

Figure 4. Variable-temperature ^{13}C NMR spectra of $Os_3(CO)_{10}$(*i*-Pr-DAB(4e)) (**1b**).

In analogy to the assignment for $Os_3(CO)_{10}(1,1\text{-}Ph_2P(CH_2)_2PPh_2)$ and $Os_3(CO)_{10}(1,1\text{-}PMe_2Ph)_2$ (Table X) the lowest field peak in the 193 K ^{13}C NMR spectrum of **1b** belongs very likely to the two CO ligands a and a′ (Scheme II) which are both linked to Os(1) to which also the R-DAB ligand is chelate bonded.[28] This type of CO groups shows in the case of the phosphine compounds coupling with two equivalent P ligands. The signals at 184.0 (b, b′) and 182.9 ppm (c, c′) are assigned to the four axial CO ligands on Os(2) and Os(3) again in analogy to the assignment of $Os_3(CO)_{10}(1,1\text{-}PMe_2Ph)_2$ and $Os_3(CO)_{10}(1,1\text{-}Ph_2P(CH_2)_2PPh_2)$. This is reasonable, since axial CO groups generally resonate at lower fields than the equatorial CO groups.[29] Finally, the signals at 174.3 and 169.8 ppm are assigned to the equatorial CO groups (e, e′) and (d, d′), respectively. This is different from the assignment for both phosphine compounds for which the lowest resonance is about 179 ppm was assigned to dd′ and the highest one to ee′ (see Table X). However, it should be noted that the five ^{13}CO signals of $Os_3(CO)_{10}(\eta^4$-cyclohexa-1,3-diene) at −40 °C were assigned in a very similar way (Table X) with the single exception that here the (a, a′) signal appears at higher field (181.8 ppm) than those of the CO signals of the axial CO groups on Os(2) and Os(3). The latter difference can easily be explained, since it is known for also (L-L)$Fe(CO)_3$ that the ^{13}CO signals in the series L-L is bipyridine, $Me_2P(CH_2)_2PPh_2$, *i*-Pr-DAB, and η^4-butadiene shift upfield from 222.3 ppm for (bpy)$Fe(CO)_3$[30] and 221.5 ppm for $(Me_2P(CH_2)_2PPh_2)Fe(CO)_3$[31] to 215.5 ppm for (i-Pr-DAB)$Fe(CO)_3$[32] and to 209 and 211.7 ppm for (η^4-butadiene)$Fe(CO)_3$.[31] The reasons for this order is not clear, but it appears that the ^{13}CO signals shift upfield with increasing π-acceptor capacity of the L-L ligand.

Scheme III. Proposed Mechanism of Exchange in the Temperature Range 203–273 K

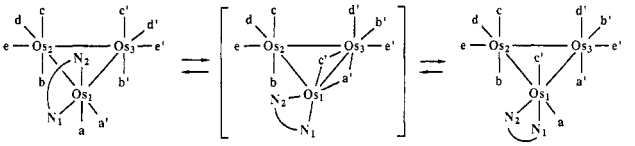

After having rationalized the chemical shift assignment, it is of interest to consider the fluxional processes in which isomer **1b** is involved. Unfortunately it was not possible to reach the slow-exchange situation due to crystallization problems. Nonetheless, it is very likely that the existence of five sharp signals and the magnetic equivalence of the *i*-Pr substituents at 193 K indicate that the compound is in the limit of fast exchange of a process which creates a mirror plane on the NMR time scale perpendicular to the Os_3 plane and which runs through Os(1) and the midpoint of the Os(2)–Os(3) bond. Therefore, we propose a process which involves a rocking of the R-DAB ligand above the plane of the osmium triangle about one axial and two equatorial coordination positions on the Os(1) atom. This process (Scheme II) is completely analogous to the one proposed for the isostructural $Os_3(CO)_{10}(\eta^4$-cyclohexa-1,3-diene) which causes the coalescence of nine ^{13}CO signals to five of relative intensity 1:1:1:1:1 (see also Table X).

At temperatures of about 203 K the signals at 188.2, 184.0, 182.9, and 169.8 ppm start to broaden and finally to coalesce to one peak at 180.9 ppm at the weighted average at 293 K, while the resonance at 174.3 ppm belonging to CO groups e and e′ remained sharp. This can only be understood if one assumes the occurrence of a process

(28) It should be noted that both phosphorus atoms in $Os_3(CO)_{10}$(diphos) and in $Os_3(CO)_{10}(PMe_2Ph)_2$ are in equatorial positions while the CO groups a and a′ reside in axial positions. However, for the assignment of a and a′ this difference is not really essential.

(29) Aime, S.; Milone, L. *Prog. Nucl. Magn. Reson. Spectrosc.* **1977**, *11*, 183.

(30) Frühauf, H. W. *J. Chem. Res., Miniprint* **1983**, 2035.

(31) Mann, B. E. *Adv. Organomet. Chem.* **1974**, *12*, 135.

(32) Frühauf, H. W.; Breuer, J. *J. Organomet. Chem.* **1984**, *277*, C13.

Scheme IV. Proposed Mechanism for the Formation of $Os_3(CO)_{10}$(R-DAB(4e)) (1) and $Os_3(CO)_{10}$(R-DAB(6e)) (2)

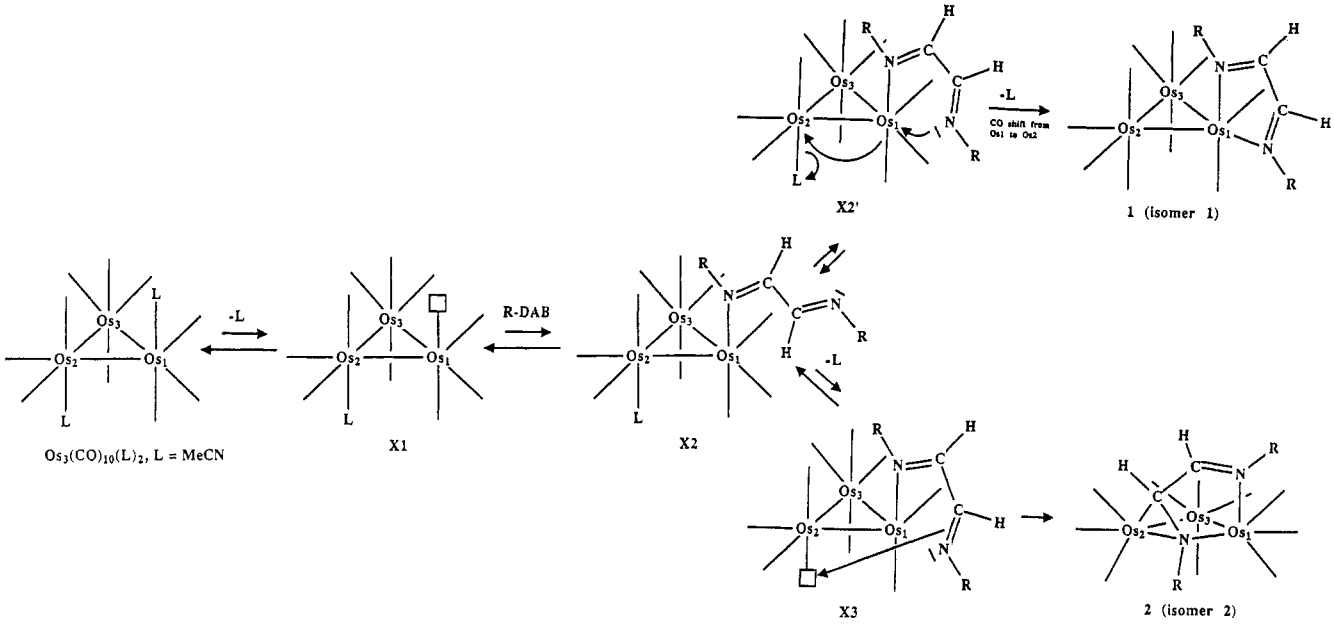

which exchanges via pairwise bridge–terminal CO interchanges, e.g., the CO groups a or a′ with b′, d′ and c′ and at the same time a or a′ with b, d and c (Scheme III). This type of process which is well-known for other compounds[27,33-35] must occur perpendicular to the Os_3 plane and is not blocked by the R-DAB ligand, since this ligand is already involved in a rocking motion causing the axial–equatorial exchange of CO groups a and a′. We can thus understand that the ^{13}CO signal (e, e′) at 174.3 ppm remains sharp, since these CO groups are not involved in the exchange. The intermediate that we propose (Scheme III) is very similar to the solid-state structure of $Ru_3(CO)_{10}$(bpy),[17] which is reasonable, since the energy difference between this structure and the structure of **1b** is expected to be small. Also it is evident from the crystal structure of **1b** that there is a tendency for the axial CO groups (C2, C4, C6, C8, and C9; Figure 1) toward a semibridging position, which facilitates pairwise terminal–bridge CO exchange process. It should be noted that the concentration of the intermediate is very small, since the IR spectra in the solid state and and at 148 K in pentane are virtually identical with the room-temperature spectra which are in full accord with the solid-state structure of **1b** with axial–equatorial coordination of R-DAB.

At still higher temperatures the signal at 174.3 ppm (e, e′) and the coalesced signal at 180.9 ppm start to coalesce to one signal at 308 K at 180.3 ppm, which is at about the weighted average. Various processes and/or combinations of processes may explain this coalescence. It is likely that in this temperature range the CO groups start to exchange in the equatorial plane as proposed by Lewis et al.[25] In addition axial–equatorial exchange of CO groups on Os(2) and Os(3) may also occur.

Reaction Mechanism of the Reaction of $Os_3(CO)_{10}(MeCN)_2$ with R-DAB. An intriguing aspect of the reaction of $Os_3(CO)_{10}(MeCN)_2$ with R-DAB is the formation of two isomers of $Os_3(CO)_{10}$(R-DAB) of which the ratio is mainly dependent on the R group and to some extent also on the type of solvent.

The influence of the R group on the product formation may be understood by considering the steric bulk of the R group. In the past the steric aspects of the R substituents on the product formation of the $Ru_3(CO)_{12}$/R-DAB reaction system have been investigated. Certain trends have been established, and it is now understood that very bulky R substituents block the approach of the π-bonds of the N=CC=N skeleton, thereby hindering the η^2-C=N coordination and favoring σ,σ-N,N′ chelate bonding. For Ru it was found that, for example, σ,σ-N,N′ chelate bonding occurs preferentially for R = 2,4,6-mesityl and *o*-xylyl, while σ-N, μ_2-N′, η^2-C=N′ (6e) coordination has been observed for *i*-Pr, c-Hex, c-Pr, and even *t*-Bu.[2] These rules are not strictly adhered to, since the R groups favoring 6e donation may also give σ,σ-N,N′, η^2,η^2-C=N,-C′=N′ (8e) coordination.[36] In view of these results it is not surprising that the small c-Pr group tends to 6e-donor type of bonding, while the largest group in our study, i.e. R = neo-Pent, appears to give in the case of Os a 4e-chelate type of bonding. It should be noted that in the case of Ru the neo-Pent group may occur in the 6e- or 8e-donor type of bonding, which underlines that steric factors may differ from metal to metal, while also the size of the cluster may be important. Finally, in this study for R = *i*-Pr the R-DAB ligand may give both types of bonding, while in this case the type of product is dependent on the solvent. Until now solvent dependence on the product formation has not been observed in R-DAB chemistry.

The role of solvents on reactions are generally little understood because of the many factors involved that complicate the evolution of a clear picture. However, it seems worthwhile to devote some discussion to the observation that **1b** is the main product in MeCN and THF and **2b** is formed predominantly in toluene. In the first case excess *i*-Pr-DAB is necessary, while in the last reaction 1 equiv of *i*-Pr-DAB is sufficient in the reaction with $Os_3(CO)_{10}(MeCN)_2$. Therefore, we assume the presence of the equilibrium between $Os_3(CO)_{10}(MeCN)_2$ and $Os_3(CO)_{10}(MeCN)$ (X1, Scheme IV) which lies far to the side of the bis(acetonitrile) complex.[10b,37] The intermediate

(33) Forster, A.; Johnson, B. F. G.; Lewis, J.; Matheson, T. W.; Robinson, B. H.; Jackson, W. G. *J. Chem. Soc., Chem. Commun.* **1974**, 1042.
(34) Johnson, B. F. G.; Lewis, J.; Reichert, B. E.; Schorpp, K. T. *J. Chem. Soc., Dalton Trans.* **1976**, 1403.
(35) Deeming, A. J.; Donovan-Mtunzi, S.; Kabir, S. E. *J. Organomet. Chem.* **1985**, *281*, C43.
(36) Adams, R. D. *J. Am. Chem. Soc.* **1980**, *102*, 7476.

X1, however, should occur in higher concentrations in toluene than in acetonitrile because of the mentioned equilibrium, which explains that in acetonitrile as solvent an excess of *i*-Pr-DAB is needed for the reaction to proceed. Subsequently the *i*-Pr-DAB ligand may then occupy the vacant coordination position in a σ-N monodentate coordinated fashion to give $Os_3(CO)_{10}(MeCN)(\sigma$-N-*i*-Pr-DAB(2e)) (X2, Scheme IV).[38] A few complexes with R-DAB in the 2e σ-N coordination mode are known.[2] From this point the reaction may proceed in two directions.

In toluene it is to be expected that some solvent assisted dissociation of the second acetonitrile in the intermediate X2 may take place to give the coordinatively unsaturated $Os_3(CO)_{10}(\sigma$-N-*i*-Pr-DAB(2e)) (X3) with the vacant position (possibly filled by toluene) on Os(2). The noncoordinated end of the *i*-Pr-DAB molecule may then become attached via its σ-C=N bond to Os(2) with the formation of **2b**. Since the μ_2-N′, η^2-C=N′ bonded moiety donates four electrons, the Os(1)–Os(2) bond will be ruptured. Such an intramolecular pathway as described above is attractive, since it should be a facile process which explains that the reactions already proceeds at temperatures of about 20 °C. The second pathway that takes place in acetonitrile and THF for *i*-Pr-DAB at 45 °C and room temperature, respectively, is slightly different in the sense that the noncoordinated side of *i*-Pr-DAB in X2′, with a cis conformation around the central C–C′ bond of the R-DAB ligand, substitutes a CO group on Os(1). This CO group moves via bridging positions between Os(1) and Os(2) to substitute the remaining acetonitrile ligand on Os(2), thereby forming **1b** with *i*-Pr-DAB bonded as a chelate.[39,40]

The two pathways described above for the reactions of $Os_3(CO)_{10}(MeCN)_2$ with *i*-Pr-DAB differ only slightly, and furthermore the small differences in reaction temperatures indicate small energy differences. This is further underscored by the fact that both pathways may occur in both toluene and acetonitrile. For example, the reaction of $Os_3(CO)_{10}(MeCN)_2$ with c-Pr-DAB gave at 45 °C **2a**, while for R = neo-Pent in toluene at 20 °C **1c** was obtained. This of course demonstrates the dominance of the steric bulk of R over the lesser influences exerted by the solvents.[41]

We can exclude that **1b**, in the reaction of *i*-Pr-DAB with $Os_3(CO)_{10}(MeCN)_2$, is an intermediate in the formation of **2b**. This is evidenced by the fact that at room temperature both isomers are stable in solution and do not interconvert. This evidence is strengthened by the observation that only at 65 °C in nonane **1b** started to be converted to **2b** with concomitant formation of **3b**.[12] This result shows that for R = *i*-Pr the σ,σ-N,N′ R-DAB bonded isomer is thermodynamically less stable than the σ-N, μ_2-N′, η^2-C=N′ bonded isomer. Since this thermodynamically more stable isomer is formed at lower temperatures (20 °C) than the σ,σ-N,N′ R-DAB isomer (45 °C), it is unlikely that the latter compound acts as an intermediate in the reaction sequence taking place for R = *i*-Pr in toluene at 20 °C.

An interesting aspect of the reaction system is that contrary to general experience in the osmium carbonyl chemistry the Os–Os bonding may be ruptured easily if the right pathway is chosen. Other examples of facile Os–Os bond breaking are the reaction of $Os_3(CO)_{10}(MeCN)_2$ with dimethyl azodicarboxylate and with 2-ethenylpyridine in toluene at room temperature which gave the unfolded clusters $Os_3(CO)_{10}(MeO_2CN{=}NCO_2Me)$[20] and $HOs_3(CO)_{10}(NC_5H_4CH{=}CH)$,[14,42] respectively, and further the reaction of allene with $Os_3(CO)_{11}(MeCN)$ at room temperature which afforded $Os_3(CO)_{10}(C(CH_2)_2)$[20] which contains one nonbonded Os_2 pair. These reactions indicate that with well-chosen compounds and reaction conditions Os–Os bonds may be more readily cleaved than originally supposed.[43,44]

Acknowledgment. We thank J. M. Ernsting for his assistance with the recording of the NMR spectra, Prof. C. W. Hilbers for the measuring time on a Bruker AM500 spectrometer, E. Kluft and G. U. A. Sai for recording the mass spectra, and Prof. A. J. Deeming, Dr. C. J. Elsevier, Dr. H. W. Frühauf, and Dr. D. J. Stufkens for stimulating discussions. We thank the Netherlands Foundation for Chemical Research (S.O.N.) and the Netherlands Organization For Pure Research (Z.W.O.) for their financial support.

Supplementary Material Available: A listing of elemental analysis data and listings of anisotropic thermal parameters of the non-hydrogen atoms and stereo ORTEP views for **1b** and **2a** (5 pages); listings of structure factor amplitudes for **1b** and **2a** (36 pages). Ordering information is given on any current masthead page.

(37) The intermediate X1 was also proposed in investigations of the substitution kinetics of $Os_3(CO)_{10}(MeCN)_2$ with phosphorus donor ligands. Dahlinger, K.; Poë, A. J.; Sayal, P. K.; Sekhar, V. C. *J. Chem. Soc., Dalton Trans.* **1986**, 2145.

(38) It has been attempted to react $Os_3(CO)_{11}(MeCN)$ with R-DAB in acetonitrile, toluene, and benzene. Although in all cases a reaction was observed at higher temperatures, neither the two isomers of $Os_3(CO)_{10}$(R-DAB) nor the complex $Os_3(CO)_{11}$(R-DAB) were formed.

(39) It is not really necessary to have first MeCN loss in this process since also one Os–Os bond may be cleaved, giving an intermediate with a chelating R-DAB ligand and a CO group bridging an nonbonded Os···Os pair.

(40) Such a monodentate–chelating conversion is not uncommon as indicated by the temperature-dependent ^{1}H NMR studies of *trans*-$PdCl_2(PPh_3)(\sigma$-N-*t*-Bu-DAB(2e)), which shows the occurrenceof a fluxional process involving the reversible conversion of the R-DAB ligand from the σ-N monodentate R-DAB mode of bonding to an intermediate with chelate bonding. van Koten, G.; van der Poel, H.; Vrieze, K. *Inorg. Chem.* **1980**, *19*, 1145.

(41) Another example of this is the reaction of $Os_3(CO)_{10}(MeCN)_2$ with RCH=CHC(O)Me to give $HOs_3(CO)_{10}(RC{=}CHC(O)Me)$.[14] When R = H, a product with a coordinated alkene function and two metal–metal bonds was formed while with R = Me a compound with a closed polyhedron and a noncoordinated alkene function was found.

(42) This compound is of special interest because one of the main differences between vinylpyridine and R-DAB is the absence of the second nitrogen lone pair in the former ligand which keeps both ends of the metal triangle together in the R-DAB complex.

(43) Connor, J. A. In *Transition Metal Clusters*, Johnson, B. F. G., Ed.; Wiley: New York, 1980; p 345.

(44) Albers, M. O.; Robinson, D. J. *Coord. Chem. Rev.* **1986**, *69*, 127.